A method for numerical modelling of convection-reaction-diffusion using electrical analogues

Sabawoon Shafaq, Alan Kennedy and Yan Delauré

School of Mechanical and Manufacturing Engineering, Dublin City University, Glasnevin, Dublin 9, Ireland

Abstract

In this paper, a new method, called the Lumped-component Circuit Method (LCM), is developed for one- and two-dimensional convection-reaction-diffusion with low to moderate Peclet numbers, tested for modelling both steady-state and transient problems, and compared to standard FVM schemes. The method has been developed principally for solving equations with piecewise-constant coefficients using nodes that are not positioned to correspond to the coefficient discontinuities. In such situations, the FVM solutions do not converge consistently as the node spacing is decreased, but LCM solutions do. In general, the LCM method is more accurate than the FVM schemes tested, and, while the computational cost of LCM is higher, results suggest that it can be more efficient. Like the Transmission Line Method (TLM), it is an indirect scheme in which the problem to be solved is first represented by an analogous transmission line (TL). Unlike with TLM, however, the TL is then modelled using a lumped-component circuit, the voltages at nodes within that circuit being calculated.

Introduction

The development of efficient, reliable and accurate numerical methods for the solution of convection-reaction-diffusion equations (CRDEs) is ongoing, especially for certain types of problems, because they occur in the modelling of a very broad range of processes. They describe phenomena in chemistry [1], biology [2], semiconductor physics [3-4], ecology [5], finance [6-7], computational fluid dynamics [8-9] and other fields. A broad range of numerical methods already exist that can be used to estimate solutions of CRDEs [10-11], with significant variation in accuracy, consistency and computational cost [12].

The CRDE, which accounts for the three processes of convection, reaction and diffusion, can be derived using conservation principles from the Reynolds transport equation [12-13]. The concentration of the diffusant, ϕ, is governed by

$$\frac{\partial \phi}{\partial t} = \nabla \cdot \left(D \nabla \phi \right) - \nabla \cdot \left(\mathbf{v} \phi \right) - K\phi + S \tag{1.1}$$

where the coefficients of diffusivity, D, convection, $\mathbf{v}$, reaction, K, and source term, S, may all depend on space, time and/or ϕ. Only linear problems with piecewise-constant coefficients are considered here. Such problems occur, for example, where the problem domain includes two or more physical media through which the diffusant moves. An example is the purification and separation of organic compounds by passing them through different media [14-15]. Other examples include the modelling of semiconductor drift-diffusion [4], injection-moulding [16] and multiphase fluid flow [8, 15, 17].

The Lumped-component Circuit Method (LCM) solves CRDEs with convection terms expressed in non-conservative form, i.e. of the form

$$\frac{\partial \phi}{\partial t} = \nabla \cdot \left(D \nabla \phi \right) - \mathbf{v} \cdot \nabla \phi - K\phi + S \tag{1.2}$$

but could be used to solve CRDEs with conservative convection terms (as in Eq. (1.1)), for example, in one dimension, by adding dv/dx to the reaction coefficient K.

The method is based on the fact that the equation for the voltage along a length of transmission line (TL), i.e. a pair of parallel conductors, can have the same form as a CRDE. A series of connected TL sections can act as an analogue for a one-dimensional convection-reaction-diffusion problem with piecewise-constant coefficients.

LCM is very similar to the transmission line method (TLM) in that it seeks a solution for the CRDE by solving the voltage along a transmission line whose equation is analogous to the CRDE [18], however, unlike in TLM, the transmission line that is modelled has zero inductance and is, itself, modelled using a lumped component circuit.

The method in one dimension

Consider a one-dimensional problem with distinct homogeneous physical media as represented in Figure 1(a). The corresponding CRDE (with non-conservative convection term) is

$$\frac{\partial \phi}{\partial t} = \frac{\partial}{\partial x}\left(D_i \frac{\partial \phi}{\partial x}\right) - K_i \phi - v_i \frac{\partial \phi}{\partial x} + S_i \text{ , } x_{mi} < x < x_{m(i+1)} \tag{1.3}$$

where the values of x_{mi} indicate the positions of the interfaces as shown in the diagram. Figure 1(b) represents a series of connected transmission line sections, the distributed resistance, capacitance, shunt conductance (i.e. the conductance per unit length between the two conductors that form the TL) and source current (i.e. the current per unit length from a current source distributed along the TL length) of section *i* being given by the functions $R_{di}(x)$, $C_{di}(x)$, $G_{di}(x)$ and $I_{di}(x)$, respectively. The ends of the TL sections correspond to the discontinuities in the problem being solved. The voltage along such a TL is governed by (see Appendix A)

$$\frac{\partial V}{\partial t} = \frac{\partial}{\partial x}\left(\frac{1}{R_{di} C_{di}} \frac{\partial V}{\partial x}\right) - \frac{G_{di}}{C_{di}} V - \frac{1}{R_{di}} \frac{\partial}{\partial x}\left(\frac{1}{C_{di}}\right) \frac{\partial V}{\partial x} + \frac{I_{di}}{C_{di}} \text{ , } x_{mi} < x < x_{m(i+1)} \tag{1.4}$$

Equations (1.3) and (1.4) are equivalent if the TL section properties satisfy

$$R_{di} C_{di} = 1/D_i \text{ , } \frac{1}{R_{di}} \frac{\partial}{\partial x}\left(\frac{1}{C_{di}}\right) = v_i \text{ , } \frac{G_{di}}{C_{di}} = K_i \text{ , } \frac{I_{di}}{C_{di}} = S_i \tag{1.5}$$

Combining two of these conditions gives

$$\frac{v_i}{D_i} = C_{di} \frac{d}{dx}\left(\frac{1}{C_{di}}\right)$$

which, when solved, gives

$$1/C_{di} = c_{i-1} \exp\left[\left(x - x_{mi}\right) v_i / D_i\right],\ x_{mi} < x < x_{m(i+1)}$$

where $c_{i-1} = 1/C_d(x_{mi})$, i.e. one over the distributed capacitance at the start of TL section *i*. From Eq. (1.5), the other distributed properties must also vary exponentially over space. A TL section with such properties is referred to here as an "exponential TL section".

Now, in convection-reaction-diffusion with a non-conservative convection term, the flux due to diffusion must be the same on either side of a discontinuity (as opposed to the flux due to the combination of diffusion and convection which must be conserved if the CRDE has a conservative convection term) [19]. The diffusive flux is given by Fick's Equation and so, for example, at $x = x_{m2}$,

$$D_1 \left.\frac{\partial \phi}{\partial x}\right|_{xl} = D_2 \left.\frac{\partial \phi}{\partial x}\right|_{xr}$$

where *xl* indicates the point just to the left of $x = x_{m2}$ and *xr* indicates the point just to the right. Similarly, for the analogous transmission line at that point, the current to the left of the discontinuity must equal the current to the right. From Eq. (A.3) that gives

$$\frac{1}{R_{d1}\left(x_{m2}\right)} \left.\frac{\partial V}{\partial x}\right|_{xl} = \frac{1}{R_{d2}\left(x_{m2}\right)} \left.\frac{\partial V}{\partial x}\right|_{xr}$$

Since, the derivatives of ϕ must equal the derivatives of V, the TL can only be an exact analogue of the convection-reaction-diffusion problem if

$$\frac{R_{d2}\left(x_{m2}\right)}{R_{d1}\left(x_{m2}\right)} = \frac{D_1}{D_2}$$

Since, at any point, $R_{di}(x) C_{di}(x) = 1/D_i$, it is clear that this requires that $C_{d2}(x_{m2}) = C_{d1}(x_{m2})$. The same is true for all other discontinuities (i.e. the value of the distributed capacitance of the transmission line must be continuous along its length). This allows c_i (the value of one over the distributed capacitance at the start of exponential TL section i) to be written in terms of c_{i-1}

$$c_i = c_{i-1} \exp\left[\left(x_{m(i+1)} - x_{mi}\right) v_i \big/ D_i\right] \tag{1.6}$$

where c_1 can be any non-zero value.

If the distributed properties of the TL sections in Figure 1(b) satisfy the equations above, then the TL is an exact analogue of the problem represented in Figure 1(a). The next step is to position nodes and then model the lengths of transmission line between adjacent nodes using lumped-component circuit elements (LCEs). For an exact model, each LCE must behave in the same way as the equivalent length of TL, but only in terms of the currents and voltages at either end (since results are only calculated at the nodes). A lumped-component circuit cannot, with a finite number of components, model a length of TL exactly in the time-domain. A simple LCE can, however, model a length of TL exactly under steady-state conditions. As shown below, each LCE can then be adjusted so that it can approximate a length of TL under transient conditions.

The positioning of the nodes splits the TL into exponential TL segments as shown in Figure 1(c). The numbering of these segments is indicated in the diagram, as is the notation for the length of a segment (e.g. $l_{4,3}$ is the length of the third segment, counting from the left, between nodes 4 and 5). The I/O relationship (i.e. the relationship between the output, or right-hand end, current and voltage and the input, or left-hand end, current and voltage) for each exponential TL segment can be found. From those, the I/O relationships for the "compound sections" between each pair of adjacent nodes, as indicated in Figure 1(d), can be calculated. Once they are known, equivalent LCEs (as represented in Figure 1(e)) can be found. These can exactly model the TL, and hence the CRDE, under steady-state conditions. For transient modelling, the capacitance of these circuit elements must be calculated so that they approximate the TL compound sections. Once boundary conditions are implemented, it is then straightforward to calculate the voltages at the nodes (i.e. the approximation of the solution of the original problem) in the lumped-component circuit over time.

As mentioned above, the first step in deriving the equations for the method is to find the relationship between the inputs and the outputs for a general TL segment numbered n,j under steady-state conditions. As shown in Appendix B, it is

$$\begin{bmatrix} V_{o|n,j} \\ I_{o|n,j} \end{bmatrix} = \mathbf{A}_{\mathbf{TL}}^{n,j} \begin{bmatrix} V_{i|n,j} \\ I_{i|n,j} \end{bmatrix} + \mathbf{b}_{\mathbf{TL}}^{n,j} \tag{1.7}$$

where the TL "I/O matrices" are

$$\mathbf{A}_{\mathbf{TL}}^{n,j} = \begin{bmatrix} \beta_{n,j}\delta_{n,j} - \dfrac{\beta_{n,j}\gamma_{n,j}v_{n,j}}{\zeta} & -\dfrac{2c_{n,j}\beta_{n,j}\gamma_{n,j}}{\zeta_{n,j}} \\ -\dfrac{2D_{n,j}K_{n,j}\gamma_{n,j}}{c_{n,j}\beta_{n,j}\zeta_{n,j}} & \dfrac{\gamma_{n,j}v_{n,j} + \delta_{n,j}\zeta_{n,j}}{\beta_{n,j}\zeta_{n,j}} \end{bmatrix},\ \mathbf{b}_{\mathbf{TL}}^{n,j} = \begin{bmatrix} \dfrac{\zeta_{n,j} + \beta_{n,j}\gamma_{n,j}v_{n,j} - \beta_{n,j}\delta_{n,j}\zeta_{n,j}}{K_{n,j}\zeta_{n,j}} \\ \dfrac{2D_{n,j}\gamma_{n,j}}{c_{n,j}\beta_{n,j}\zeta_{n,j}} \end{bmatrix} S_{n,j} \tag{1.8}$$

where $c_{n,j}$ is the value if $1/C_{dn,j}$ at the left-hand end of the segment, $\beta_{n,j} = \exp\left(v_{n,j} \big/ 2D_{n,j}\, l_{n,j}\right)$, $\zeta_{n,j} = \sqrt{v_{n,j}^2 + 4K_{n,j}D_{n,j}}$, $\gamma_{n,j} = \sinh\left(\zeta_{n,j} \big/ 2D_{n,j}\, l_{n,j}\right)$, $\delta_{n,j} = \cosh\left(\zeta_{n,j} \big/ 2D_{n,j}\, l_{n,j}\right)$, and $D_{n,j}$, $v_{n,j}$, $K_{n,j}$ and $S_{n,j}$ are the problem coefficients corresponding to that segment. Equivalent equations are given in Appendix C for situations where $K_{n,j}$ is zero, or both $v_{n,j}$ and $K_{n,j}$ are zero.

Eq. (1.7) is for a single segment in a compound section. A similar relationship can be found for a compound section with multiple segments. To understand how that is done, first consider compound section 2 in Figure 1(d) composed of two segments. Eq. (1.7) gives

$$\begin{bmatrix} V_{o|2,1} \\ I_{o|2,1} \end{bmatrix} = \mathbf{A}_{\mathrm{TL}}^{2,1} \begin{bmatrix} V_{i|2,1} \\ I_{i|2,1} \end{bmatrix} + \mathbf{b}_{\mathrm{TL}}^{2,1},\ \begin{bmatrix} V_{o|2,2} \\ I_{o|2,2} \end{bmatrix} = \mathbf{A}_{\mathrm{TL}}^{2,2} \begin{bmatrix} V_{i|2,2} \\ I_{i|2,2} \end{bmatrix} + \mathbf{b}_{\mathrm{TL}}^{2,2} \tag{1.9}$$

Since $V_{o|2,1} = V_{i|2,2}$ and $I_{o|2,1} = I_{i|2,2}$, these can be combined to give the I/O relationship for the compound section

$$\begin{bmatrix} V_{o|2,2} \\ I_{o|2,2} \end{bmatrix} = \mathbf{A}_{\mathrm{TL}}^{2,2}\mathbf{A}_{\mathrm{TL}}^{2,1} \begin{bmatrix} V_{i|2,1} \\ I_{i|2,1} \end{bmatrix} + \mathbf{A}_{\mathrm{TL}}^{2,2}\mathbf{b}_{\mathrm{TL}}^{2,1} + \mathbf{b}_{\mathrm{TL}}^{2,2} \tag{1.10}$$

The I/O relationship for a more general compound section with N_n segments between nodes n and $n+1$ is

$$\begin{bmatrix} V_{n+1} \\ I_{n+1} \end{bmatrix} = \mathbf{A}^{\mathrm{CS}.n}_{\mathbf{TL}} \begin{bmatrix} V_n \\ I_n \end{bmatrix} + \mathbf{b}^{\mathrm{CS}.n}_{\mathbf{TL}} \tag{1.11}$$

where V_n and I_n are the voltage and current at node n and

$$\mathbf{A}^{\mathrm{C.S.n}}_{\mathrm{TL}} = \prod_{j=N_n}^{1} \mathbf{A}^{n,j}_{\mathrm{TL}}, \quad \mathbf{b}^{\mathrm{CS.n}}_{\mathrm{TL}} = \left(\sum_{j=2}^{N_n} \mathbf{A}^{n,j}_{\mathrm{TL}} \mathbf{b}^{n,j\text{-}1}_{\mathrm{TL}} \right) + \mathbf{b}^{n,N_n}_{\mathrm{TL}} \tag{1.12}$$

The next step is to find an LCE to link nodes n and n+1 that has an equivalent steady-state I/O relationship. Such a circuit is shown in Figure 2. The net currents entering nodes n and n+1 must both be zero giving

$$I_n - G_{l,n} V_n + I_{l,n} + \frac{V_{n+1} - V_n}{R_n} = 0 \tag{1.13}$$

and

$$\frac{V_n - V_{n+1}}{R_n} + I_{r,n} - G_{r,n} V_{n+1} - I_{n+1} = 0 \tag{1.14}$$

Solving these for V_{n+1} and I_{n+1} gives

$$\begin{bmatrix} V_{n+1} \\ I_{n+1} \end{bmatrix} = \mathbf{A}^{n}_{\mathbf{LC}} \begin{bmatrix} V_n \\ I_n \end{bmatrix} + \mathbf{b}^{n}_{\mathbf{LC}} \tag{1.15}$$

where the LCE I/O matrices are

$$\mathbf{A}^{n}_{\mathbf{LC}} = \begin{bmatrix} G_{l,n} R_n + 1 & \text{-}R_n \\ \text{-}G_{l,n} \left(G_{r,n} R_n + 1 \right) \text{-} G_{r,n} & G_{r,n} R_n + 1 \end{bmatrix}, \; \mathbf{b}^{n}_{\mathbf{LC}} = \begin{bmatrix} \text{-}R_n I_{l,n} \\ I_{r,n} + \left(G_{r,n} R_n + 1 \right) I_{l,n} \end{bmatrix}$$

Equations (1.11) and (1.15) both have the same form. In order for the lumped-component circuit element connecting nodes n and n+1 to be equivalent to the corresponding compound TL section, the component parameters must be such that $\mathbf{A}^{n}_{\mathrm{LC}} = \mathbf{A}^{\mathrm{CS}.n}_{\mathrm{TL}}$ and $\mathbf{b}^{n}_{\mathrm{LC}} = \mathbf{b}^{\mathrm{CS}.n}_{\mathrm{TL}}$, giving

$$R_n = -\mathrm{A}^{\mathrm{CS}.n}_{\mathrm{TL}1,2}, \; G_{l,n} = -\frac{\mathrm{A}^{\mathrm{CS}.n}_{\mathrm{TL}\,1,1} - 1}{\mathrm{A}^{\mathrm{CS}.n}_{\mathrm{TL}\,1,2}}, \; G_{r,n} = -\frac{\mathrm{A}^{\mathrm{CS}.n}_{\mathrm{TL}\,2,2} - 1}{\mathrm{A}^{\mathrm{CS}.n}_{\mathrm{TL}\,1,2}}, \; I_{\mathrm{l},n} = \frac{\mathrm{b}^{\mathrm{CS}.n}_{\mathrm{TL}\,1,1} - 1}{\mathrm{A}^{\mathrm{CS}.n}_{\mathrm{TL}\,1,2}}, \; I_{r,n} = \frac{\mathrm{b}^{\mathrm{CS}.n}_{\mathrm{TL}\,2,1} - \mathrm{b}^{\mathrm{CS}.n}_{\mathrm{TL}\,1,1} \big/ \mathrm{A}^{\mathrm{CS}.n}_{\mathrm{TL}\,1,2}}{\mathrm{A}^{\mathrm{CS}.n}_{\mathrm{TL}\,2,2}} \tag{1.16}$$

Once these values are calculated, and boundary conditions implemented, the full steady-state lumped-component circuit (as represented in Figure 1(e)) can be modelled in order to calculate the node voltages (i.e. the solution of the CRDE at those points). Only Dirichlet boundaries are implemented here in which the voltages at the boundary nodes are simply fixed at the desired values.

As mentioned above, for transient modelling, capacitance must be added to the LCEs. This is done by adding two capacitors to each LCE. Two such LCEs are shown in Figure 3, and the values of the capacitances are given below. The next step is to determine the node voltage at any node n in terms of the voltages at the surrounding nodes.

The net current entering node n is zero, and so

$$\left(C_{r,n\text{-}1} + C_{l,n} \right) \frac{\partial V_n}{\partial t} = \left(\frac{V_{n+1} - V_n}{R_n} \right) - \left(\frac{V_n - V_{n\text{-}1}}{R_{n\text{-}1}} \right) - V_n \left(G_{r,n\text{-}1} + G_{l,n} \right) + I_{r,n\text{-}1} + I_{l,n} \tag{1.17}$$

or, after rearranging,

$$\begin{aligned} R_{n\text{-}1} \left(C_{r,n\text{-}1} + C_{l,n} \right) \frac{\partial V_n}{\partial t} &= P_n \left(V_{n+1} - V_n \right) - \left(V_n - V_{n-1} \right) - \ldots \\ &\ldots V_n R_{n-1} \left(G_{r,n-1} + G_{l,n} \right) + R_{n-1} \left(I_{r,n-1} + I_{l,n} \right) \end{aligned} \tag{1.18}$$

where $P_n = R_{n-1}/R_n$. Note that the coefficients in Eq. (1.18) are all independent of c_1, i.e. independent of the TL distributed capacitance at $x = 0$ which, as stated above, can be chosen arbitrarily.

The capacitance values for the LCEs cannot be determined in the same way as the other circuit parameters (because an LCE cannot be equivalent to a length of TL under transient conditions). An approximation is required.

Consider how the distributed source current, $I_d(x)$, within a compound TL section is modelled by two lumped current sources at either end of the corresponding LCE. It varies in a piecewise-exponential fashion, as does the distributed capacitance, but also depends on $S(x)$, the source term being modelled. Some of the TL distributed source current flows to the right-hand end of the compound section and some flows to the left-hand end. How much reaches each end depends on the distributed resistance and shunt conductance between the nodes. The same quantities of current must be supplied by the lumped current sources in the LCE (i.e. $I_{l,n}$ and $I_{r,n}$ for LCE n) in order for it to model the TL section accurately. The relationship between $I_{l,n}$ and $I_{r,n}$ and $I_d(x)$, which depends on $S(x)$, $v(x)$, $D(x)$, etc., is derived above.

Now consider the TL distributed capacitance, $C_d(x)$. For the LCE numbered n, the currents flowing into the two lumped capacitors are $C_{l,n}dV_n/dt$ and $C_{r,n}dV_{n+1}/dt$. These must represent the current flowing from these points into the corresponding compound TL section because of the distributed capacitance in that section. The distributed capacitance can be viewed as a distributed current sink, similar to the distributed current source, but proportional to dV/dt. If it is assumed that dV/dt is a constant between nodes n and n+1 (and so $dV_n/dt = dV_{n+1}/dt$ in the corresponding LCE) then the relationship between $C_{l,n}$ and $C_{r,n}$ and $C_d(x)$ over the length of the compound TL section is similar to that between $I_{l,n}$ and $I_{r,n}$ and $I_d(x)$. In practice that will not be the case, and so each LCE can only approximate the equivalent compound section.

Given this assumption, the two lumped capacitances, for LCE n, can be calculated as

$$C_l = \frac{\mathbf{b}^{*\mathrm{CS}}_{\mathrm{TL}\,1,1} - 1}{\mathbf{A}^{*\mathrm{CS}}_{\mathrm{TL}\,1,2}}, \quad C_r = \frac{\mathbf{b}^{*\mathrm{CS}}_{\mathrm{TL}\,2,1} - \dfrac{\mathbf{b}^{*\mathrm{CS}}_{\mathrm{TL}\,1,1}}{\mathbf{A}^{*\mathrm{CS}}_{\mathrm{TL}\,1,2}}}{\mathbf{A}^{*\mathrm{CS}}_{\mathrm{TL}\,2,2}} \tag{1.19}$$

where $\mathbf{A}^{*\mathrm{CS}}_{\mathrm{TL}\,2,2}$ and $\mathbf{b}^{*\mathrm{CS}}_{\mathrm{TL}}$ are calculated in the same way as $\mathbf{A}^{\mathrm{CS}}_{\mathrm{TL}\,2,2}$ and $\mathbf{b}^{\mathrm{CS}}_{\mathrm{TL}}$ from the individual TL I/O matrices (i.e. using Eq.(1.12)) but with S_n replaced by unity in each $\mathbf{b}^{n}_{\mathbf{TL}}$.

Testing has shown that this approximation can produce highly accurate results. It is clear that as the node spacing approaches zero, errors due to this assumption also approach zero.

To summarise, the modelling process starts by placing nodes along the domain. The length of each segment, and the number of segments between each node, are determined by the positions of the nodes and the discontinuities, and the values of $c_{n,j}$ are calculated at the discontinuities and nodes. The I/O matrices, $\mathbf{A}_{\mathbf{TL}}$ and $\mathbf{b}_{\mathbf{TL}}$, are then calculated for each TL segment using Eq. (1.8). From those, $\mathbf{A}^{\mathrm{CS}.n}_{\mathrm{TL}}$ and $\mathbf{b}^{\mathrm{CS}.n}_{\mathrm{TL}}$ (and $\mathbf{b}^{*\mathrm{CS}}_{\mathrm{TL}}$ for a time-domain model) are calculated for each compound section using Eq. (1.12). The lumped-component circuit parameters are then calculated, including, for a time-domain model, the lumped capacitances, using Equations (1.16) and (1.19). Once the boundary conditions are correctly implemented, Eq. (1.18) can be solved using any standard implicit or explicit time-stepping scheme.

This method produces exact steady-state solutions, no matter how many nodes are used and where they are placed. Errors occur in time-domain solutions due to the fact that the LCEs do not exactly model the equivalent compound TL sections when the voltage varies over space and time, due to the time-stepping scheme used, and due to the initial conditions being only defined at the nodes.

As mentioned above, the coefficients in Eq. (1.18) are all independent of c_1 (i.e. one over the distributed capacitance at node 1). The equations for the method can be reformulated so that they are independent of values of C_d, and are, instead, written in terms of C_d/C_{dn-1}. That ratio is dependent on the convection velocity, the diffusion coefficient, and the distance between nodes $n-1$ and n. Those equations are not presented here.

The method in two dimensions

The equation for the voltage on a two-dimensional network of TLs

$$\frac{\partial V}{\partial t}=\frac{\partial}{\partial x}\left(\frac{1}{2R_{dx}C_d}\frac{\partial V}{\partial x}\right)+r\frac{\partial}{\partial y}\left(\frac{1}{2R_{dy}C_d}\frac{\partial V}{\partial y}\right)-\frac{1}{R_{dx}}\frac{\partial}{\partial x}\left(\frac{1}{2C_d}\right)\frac{\partial V}{\partial x}\ldots$$
$$\ldots-\frac{r}{R_{dy}}\frac{\partial}{\partial y}\left(\frac{1}{2C_d}\right)\frac{\partial V(x,y,t)}{\partial y}-\left(\frac{G_{dx}+G_{dy}r}{2C_d}\right)V+\frac{I_{dx}+I_{dy}r}{2C_d} \tag{1.20}$$

is derived in Appendix D, where $r = \Delta y/\Delta x$ (i.e. the aspect ratio of the element used in the derivation) and $C_d = C_{dx} = C_{dy}r$, where C_{dx}, R_{dx}, etc., are the properties of the horizontal lines (i.e. the ones aligned in the x-direction), and C_{dy}, R_{dy}, etc., are the properties of the vertical lines (i.e. the ones aligned in the y-direction). It is clear that this is equivalent to the 2D CRDE with non-conservative convection terms

$$\frac{\partial\phi}{\partial t}=\frac{\partial}{\partial x}\left(D_x\frac{\partial\phi}{\partial x}\right)+\frac{\partial}{\partial y}\left(D_y\frac{\partial\phi}{\partial y}\right)-v_x\frac{\partial\phi}{\partial x}-v_y\frac{\partial\phi}{\partial y}-K\phi+S \tag{1.21}$$

if

$$R_{dx}C_d=\frac{1}{2D_x},\ R_{dy}C_d=\frac{r}{2D_y},\ \frac{1}{R_{dx}}\frac{\partial}{\partial x}\left(\frac{1}{2C_d}\right)=v_x,\ \frac{1}{R_{dy}}\frac{\partial}{\partial y}\left(\frac{1}{2C_d}\right)=\frac{v_y}{r} \tag{1.22}$$

and

$$\frac{G_{dx}+G_{dy}r}{2C_d}=K,\ \frac{I_{dx}+I_{dy}r}{2C_d}=S \tag{1.23}$$

Such a network, with the horizontal and vertical lines connected at the nodes, can be used to model convection-reaction-diffusion in two-dimensions. Along a horizontal line, G_{dy} and I_{dy} both equal zero and $C_d = C_{dx}$, and so for such a line, these formulas can be rearranged giving

$$\frac{1}{R_{dx}\,C_{dx}/2}=D_x,\ (C_{dx}/2)\frac{\partial}{\partial x}\left(\frac{1}{C_{dx}/2}\right)=\frac{v_x}{D_x},\ \frac{G_{dx}}{C_{dx}/2}=K,\ \frac{I_{dx}}{C_{dx}/2}=S$$

Similarly, along a vertical line, G_{dx} and I_{dx} both equal zero, and $C_d = C_{dy}r$, and so

$$\frac{1}{R_{dy}\,C_{dy}/2}=D_y,\ (C_{dy}/2)\frac{\partial}{\partial y}\left(\frac{1}{C_{dy}/2}\right)=\frac{v_y}{D_y},\ \frac{G_{dy}}{C_{dy}/2}=K,\ \frac{I_{dy}}{C_{dy}/2}=S$$

These specify what the distributed properties of the vertical and horizontal lines must be (and how they must vary over space) so that the equation for the voltage in the network is equivalent to Equation (1.21). These relationships are similar to those derived above for 1D LCM, with one exception (the distributed capacitance on the vertical and horizontal lines must be half what it would be if those lines each represented individual 1D problems).

These equations dictate how the distributed capacitance must vary along each line in order to correctly model the required convection. Figure 4 represents part of a 2D network and indicates the notation used here; e.g., $C_{dx,n,m}$ is the distributed capacitance in the horizontal line at node n,m, and $C_{dy,n,m}$ is the distributed capacitance in the vertical line at that node. The values of the ratios $C_{dx,n,m}/C_{dx,n-1,m}$ and $C_{dy,n,m}/C_{dy,n,m-1}$ depend on the local values of the convection velocity, the diffusion coefficient and the distance between the nodes (as in one dimension). For the voltage on the network to satisfy Equation (1.20), an additional requirement

$$C_{dx,n,m}=C_{dy,n,m}r$$

must be satisfied for each node, where r, as shown below, depends on the aspect ratio of the element corresponding to the node.

Consider a model of a problem with diffusion coefficient and convection velocity values and mesh size such that the distributed capacitance ratios must be $C_{dx,n,m}/C_{dx,n-1,m}=2$ and $C_{dy,n,m}/C_{dy,n,m-1}=3$ for all nodes. The elements are square and so $C_{dx,n,m}$ must equal $C_{dy,n,m}$ at each node (i.e. $r = 1$). Figure 5(a) shows twelve nodes in the model with corresponding distributed capacitance values that satisfy all three of these requirements.

Now consider a model for a similar problem requiring $C_{dy,n,m}/C_{dy,n,m-1}=3$, and $C_{dx,n,m}=C_{dy,n,m}$ as before. The value of v_x in this example, however, varies with y requiring $C_{dx,n,2}/C_{dx,n-1,2}=4$ and $C_{dx,n,m}/C_{dx,n-1,m}=2$ elsewhere. Figure 5(b) shows values of the distributed capacitances that have the correct ratios for this problem but that do not satisfy $C_{dx,n,m}=C_{dy,n,m}r$ for all nodes. It is clear that no set of values can satisfy all three requirements in this case, and the same is true for 2D problems in general.

The solution is to consider each element individually instead of trying to create a network of lines that satisfy all the criteria required to model the given problem. For example, Figure 5(c) shows values of the distributed capacitances that satisfy all criteria for this sample problem for the element corresponding to node 2,2, while Figure 5(d) shows values that satisfy all criteria for the element corresponding to node 3,2. For each element, then, horizontal and vertical TLs can be found that model the corresponding section of the problem domain. Equivalent lumped-component circuit elements can then be found to model each section of both TLs as in the 1D scheme. The distributed capacitances of the lines (and, therefore, the lumped capacitance values in the equivalent LCEs) must be half what they would be if the lines represented one-dimensional models.

The value of r at any node is the ratio of the distributed capacitances of the two lines at that point. It is also the aspect ratio of the element used in deriving Equation (1.20) and, for a given node, must equal the aspect ratio of the element corresponding to that node. For example, for the node shown in Figure 6, the ratio must be

$$r_{n,m}=\frac{h_{y,n,m-1}+h_{y,n,m}}{h_{x,n-1,m}+h_{x,n,m}} \tag{1.24}$$

Once the LCE parameters are known, the TL network can be modelled. Consider the four lumped-component circuit elements shown in Figure 7. The sum of the currents at node n,m is zero, and so

$$\begin{aligned}C_{rx,n-1,m}+C_{lx,n,m}+C_{ry,n,m-1}+C_{ly,n,m}\frac{\partial V}{\partial t}&=\left(\frac{V_{n+1,m}-V_{n,m}}{R_{x,n,m}}\right)-\left(\frac{V_{n,m}-V_{n-1,m}}{R_{x,n-1,m}}\right)+\left(\frac{V_{n,m+1}-V_{n,m}}{R_{y,n,m}}\right)\dots\\ \dots-\left(\frac{V_{n,m}-V_{n,m-1}}{R_{y,n,m-1}}\right)&-V_{n,m}\left(G_{rx,n-1,m}+G_{lx,n,m}+G_{ry,n,m-1}+G_{ly,n,m}\right)+I_{rx,n-1,m}+I_{lx,n,m}+I_{ry,n,m-1}+I_{ly,n,m}\end{aligned} \tag{1.25}$$

or, by rearranging,

$$\begin{aligned}R_{C,n,m}\frac{\partial V}{\partial t}&=P_{x,n,m}\left(V_{n+1,m}-V_{n,m}\right)-\left(V_{n,m}-V_{n-1,m}\right)+\\ P_{y,n,m}P_{xy,n,m}&\left(V_{n,m+1}-V_{n,m}\right)-r_{n,m}\left(V_{n,m}-V_{n,m-1}\right)-R_{G,n,m}V_{n,m}+R_{I,n,m}\end{aligned} \tag{1.26}$$

where the 2D LCM coefficients are

$$P_{x,n,m}=\frac{R_{x,n-1,m}}{R_{x,n,m}},\ P_{y,n,m}=\frac{R_{y,n,m-1}}{R_{y,n,m}},\ P_{xy,n,m}=\frac{R_{x,n-1,m}}{R_{y,n,m-1}} \tag{1.27}$$

$$R_{C,n,m}=R_{x,n-1,m}\left(C_{rx,n-1,m}+C_{lx,n,m}\right)+R_{x,n-1,m}\left(C_{ry,n,m-1}+C_{ly,n,m}\right) \tag{1.28}$$

$$R_{G,n,m}=R_{x,n-1,m}\left(G_{rx,n-1,m}+G_{lx,n,m}\right)+R_{x,n-1,m}\left(G_{ry,n,m-1}+G_{ly,n,m}\right) \tag{1.29}$$

$$R_{I,n,m}=R_{x,n-1,m}\left(I_{rx,n-1,m}+I_{lx,n,m}\right)+R_{x,n-1,m}\left(I_{ry,n,m-1}+I_{ly,n,m}\right) \tag{1.30}$$

When these are calculated, Equation (1.26) can be solved over time at each node in order to solve the equivalent 2D convection-reaction-diffusion problem.

Consider the section of horizontal transmission line between nodes 2,2 and 3,2 in both Figure 5(c) and Figure 5(d). The equivalent LCE parameters for that section must first be calculated in order to calculate the 2D LCM coefficients (using Equations (1.27) to (1.30)) for both nodes 2,2 and 3,2. It is clear from Figure 5(c) and Figure 5(d), however, that the distributed capacitance of that section of line is different when considering the two nodes. That does not, however, mean that those LCE parameters must be calculated twice. Consider, for example, a situation in which they are first calculated using the values of the distributed capacitance given in Figure 5(c) (following the steps outlined above for one dimensional models) and then used in the calculation of the 2D LCM coefficients for node 2,2. When switching to consider node 3,2, given the values in Figure 5(d), the distributed capacitance of the section is reduced by a factor of 4. The LCE parameters already calculated can simply be scaled by that factor before being used in the calculation of the 2D LCM coefficients for node 3,2. The capacitance, shunt conductance and source current values must simply be reduced by a factor of 4 in this case, while the resistance values must be increased by the same factor. This means that the requirement to consider one node at a time does not significantly increase the computational cost of the scheme.

Tests

Four tests are presented here for the purposes of validating the method and comparing results obtained with those calculated using the Finite Volume Method (FVM). FVM has been chosen for comparison because the FVM and LCM equations are similar in form, FVM is well-established for solving convection-reaction-diffusion equations, and FVM is widely used for problems with discontinuous coefficients [20-21]. In FVM, when modelling problems with piecewise-constant coefficients, nodes are generally placed so that either volume faces or nodes correspond to the points of discontinuity [18-21]. In one test here, however, the FVM models are implemented with node and volume positions that do not necessarily correspond to the discontinuities (as shown in Figure 8). The FVM model coefficients at boundary faces and across volumes are calculated using harmonic mean approximations [12] (i.e. an average value of the coefficient across a volume is used as an estimate of the coefficient at the relevant midpoint).

Test 1 involves a one-dimensional transient convection-reaction-diffusion problem with piecewise-constant coefficients. The problem geometry and coefficients are represented in Figure 8. The boundary conditions are $V(0) = 25$ and $V(1) = 49$, and the initial conditions, except at the boundaries, are $V(x,\ 0) = 25$. Standard first order explicit (FTCS) time-stepping schemes are used in both LCM and FVM models with a time step length of $\Delta t = 1\times10^{-6}$. Results at $t = 0.1$ from models with 17 evenly spaced nodes are shown in Figure 9(a). The variation in the value of $V(0.5, 0.1)$ with node spacing, h, is plotted in Figure 9(b). The same data is included in Table 1 along with values of the estimated order of convergence (EOC) [22] calculated using

$$EOC = \frac{\ln\left(\left(V_h - V_{h/2}\right)\big/\left(V_{h/2} - V_{h/4}\right)\right)}{\ln 2}$$

While the LCM solutions appear to converge consistently in a second-order fashion as h approaches zero, the same is not true for the FVM solutions. That is not surprising since the nodes/elements do not correspond to the problem coefficient discontinuities. The LCM solutions are also significantly more accurate than the equivalent FVM solutions.

The approximate error in the FVM and LCM solutions (i.e. the differences between the solution values and equivalent values calculated using a very fine grid and short time step) at $x = 0.5$, calculated with $N = 17$, are plotted over time in Figure 10. The LCM error approaches zero, as expected, as the solution approaches a steady state. It is clear that the LCM solution at that point is significantly more accurate than the FVM solution over most of the solution time.

Test 2 involves a two-dimensional problem solved using an uneven grid, the grid and the problem geometry and coefficients being indicated in Figure 11(a). The grid spacing and numbers of nodes (an $N\times N$ grid) are such that there are always nodes along the line $x = 0.5$ (i.e. along the discontinuity), the horizontal node spacing to the right of $x = 0.5$ is always half that to the left, and the vertical node spacing below $y = 0.5$ is always half that above.

In two-dimensional LCM, each TL is treated as a one-dimensional model, but it must represent a two-dimensional element of the problem being solved. Coefficient values are required at every point along each TL in order to calculate the equivalent LCE parameters. Figure 12 illustrates what coefficient values have been used in the tests presented here. It shows a section of three vertical TLs with the middle one highlighted. The dashed lines indicate half way between adjacent TLs. The diffusion, convection, reaction and source term coefficients modelled by the highlighted line at the point indicated are simply the averages of those coefficients over the grey line indicated in the diagram. That allows the model, in a simple way, to account for variations in the problem coefficients between TLs.

The central difference scheme is used for approximating the convection term in the FVM models, and the diffusion coefficient at each volume boundary face is calculated as an average of the diffusion coefficients between the two adjacent nodes.

The initial and boundary conditions for the model are $V(x, y;\ 0) = 0$, $V(0, y;\ t) = 0$, $V(x, 0;\ t) = 0$, $V(1, y;\ t) = 1$ and $V(x, 1;\ t) = 1$. Time stepping is implemented using the same technique as in the previous test with a time-step length of Δt = $1{\times}10^{-6}$. The variation in the LCM and FVM estimates of $V(0.5, 0.5; 0.02)$ as the node spacing is repeatedly halved are plotted in Figure 11(b) and presented in Table 2 along with estimates of the order of the errors. This, and other similar tests not presented here, suggests that LCM solutions converge in a consistent second-order manner while the equivalent FVM solutions do not. The LCM solutions are, as in one dimension, more accurate than those obtained using the FVM scheme, especially as the solution approaches a steady state.

In Test 2, the problem coefficients are constant along each line section joining adjacent nodes (i.e. there is only one exponential TL segment in each compound section). Test 3 involves a similar problem but with the single vertical discontinuity located at $x = 0.3$, as shown in Figure 13. The problem is modelled using an even square grid. For the node spacings used, no nodes correspond to the discontinuity. Some horizontal compound sections, therefore, comprise two exponential TL segments.

The initial and boundary conditions, and the time-step used, are the same as for Test 2. LCM solution values for different node spacings are listed in Table 3 along with estimates of the order of the errors. The method again appears to converge in a consistent second-order manner. Further investigation is required to explore whether alternative averaging techniques could improve the accuracy and convergence.

These tests are for models with relatively low element Peclet numbers, defined as

$$Pe := \frac{vh}{D}$$

In practice, in many problems of interest, $v >> D$. Many numerical schemes cannot produce accurate results when element Peclet numbers are large [23-24]. If Pe values are large, then implementation of the LCM scheme, as presented here, may be problematic, because the values of c_i calculated using Equation (1.6) can exceed floating point overflow limits. It is possible to reformulate the equations for the scheme in terms of c_i / c_{i-1}, but overflow limits can still be exceeded when Pe is very large for any element. These reformulated equations are not presented here.

To examine the performance of the scheme for large element Peclet numbers, consider a one-dimensional model with h, v, D and K all constant, and with $S = 0$. Under such circumstances, Equation (1.18) can be rewritten as

$$\frac{\partial V_n}{\partial t} = f_d\left(V_{n+1} - V_{n,m}\right) + f_u\left(V_{n-1} - V_n\right) - KV_n \tag{1.31}$$

where

$$f_d = \frac{K}{\left[1 - \exp\left(\frac{Pe - Pe^*}{2}\right)\right]\left[\exp\left(\frac{Pe + Pe^*}{2}\right) - 1\right]}$$

$$f_d = \frac{K}{\exp\left(\frac{Pe^* - Pe}{2}\right) + \exp\left(\frac{-Pe^* - Pe}{2}\right) + -1 - \exp\left(-Pe\right)}$$

and

$$Pe^* = \frac{h\sqrt{v^2 + 4KD}}{D}$$

It can be shown that, for any given values of K and h, as v/D approaches infinity, f_d approaches 0 and f_u approaches v/h. Therefore, as v/D increases, Equation (1.31)approaches

$$\frac{\partial V_n}{\partial t} = v\frac{\left(V_{n-1} - V_n\right)}{h} - KV_n \tag{1.32}$$

This is a standard first-order upwind method for the CRDE with zero diffusion. Therefore, for high element Peclet numbers, the LCM scheme produces similar results to this upwind scheme (which is known to exhibit significant levels of implicit numerical diffusion [25]).

Test 4 illustrates this with a simple one-dimensional problem with $v = 50$, $K = 20$, $D = 1\times10^{-3}$, $V(0,t) = 0$, $V(1,t) = 0$, and $V(x,t) = 0$ except at $x = 0$, solved using a time step of $\Delta t = 1\times10^{-7}$.. Figure 14 (a) shows solutions obtained at $t = 0.01$ with $N = 2001$ (giving $Pe = 25$), while Figure 14(b) shows equivalent solutions calculated with $N = 81$ (giving $Pe = 625$). The solution labelled "Upwind" in Figure 14(b) has been calculated using Equation (1.32). It is clear from Figure 14 (b) that the LCM scheme exhibits greater numerical diffusion than the FVM scheme. It does not exhibit, however, the spurious oscillations visible in the FVM solution (which can be a significant problem in modelling non-linear problems [26]).

Note that the steady-state solution for 1D LCM is exact no matter what the element Peclet number is.

Discussion and conclusions

A new method has been successfully developed for the solution of convection-reaction-diffusion equations with piecewise-constant coefficients. The method is similar to TLM in that the CRDE is solved by modelling an analogous transmission line (or network of interlinked TLs). Unlike in TLM, however, the TL (or TLs) is then modelled as a lumped-component circuit. The resulting equations are similar in form to those for FVM, but, unlike with FVM, steady-state 1D LCM solutions are exact. Transient LCM solutions can also be significantly more accurate than FVM solutions, especially as they approach a steady-state. The computational cost of LCM is higher than the FVM schemes tested here, but results suggest that, for many problems, LCM is more efficient.

Solutions obtained using the FVM schemes tested do not converge consistently if the nodes are not positioned to correspond with the coefficient discontinuities. That is not the case for LCM. A modeler using the scheme could potentially, therefore, position nodes so as to minimize errors, or concentrate nodes where the values of the solution are of particular interest, without needing to take into account the positions of discontinuities, while having the benefits of consistent convergence.

Analysis of the LCM method in one dimension shows that it approaches a first-order upwind scheme as the element Peclet number approaches infinity. The results presented here (for problems with relatively low element Peclet numbers) suggest, however, that the spatial discretization error for the method is second order. Further work is required to determine analytically the nature of the errors in one and two dimensions. Transient errors occur because of differences between sections of transmission line and the lumped-component circuits used to model them. This fact may allow novel approaches to be used for error analysis.

A simple averaging of problem coefficients has been implemented here when using one-dimensional TLs to represent areas of a 2D problem. Further work is required to test whether weighted averages could produce more accurate results.

The tests presented here are limited in scope, and comparison is only made with basic FVM schemes. The potential value of this method can only be determined by further comparison, both in terms of accuracy, qualitative behaviour, and computational cost, with a wider range of methods.

There appears to be no reason why the method could not be extended to three-dimensions and to allow the modelling of a variety of boundary condition types.

Acknowledgement

Funding from the Irish Research Council for Science, Engineering and Technology (IRCSET) is gratefully acknowledged.

Appendices

Appendix A: Derivation of the equation for the voltage along a TL

Consider a short segment of TL of length Δx with its properties (i.e. distributed resistance, $R_d(x)$, shunt conductance, $G_d(x)$, capacitance, $C_d(x)$ and source current, $I_d(x)$, all per unit length and all potentially varying along its length) represented by lumped components as shown in Figure 15. The voltage drop across the segment is

$$\left(V + \frac{\partial V}{\partial x}\Delta x\right) - V = -IR_d \Delta x \tag{A.1}$$

The sum of the currents entering the point at the right-hand side must be zero, and so

$$I - G_d \Delta x V + I_d \Delta x - C_d \Delta x \frac{\partial V}{\partial t} - \left(I + \frac{\partial I}{\partial x} \Delta x \right) = 0 \tag{A.2}$$

Rearranging Eq. (A.1) gives

$$-I = \frac{1}{R_d} \frac{\partial V}{\partial x} \tag{A.3}$$

and simplifying Eq. (A.1) and dividing across by C_d yields

$$\frac{1}{R_d C_d} \frac{\partial V}{\partial x} + \frac{I}{C_d} = 0 \tag{A.4}$$

Differentiating Eq. (A.4) with respect to x gives

$$\frac{\partial}{\partial x}\left(\frac{1}{R_d C_d} \frac{\partial V}{\partial x} \right) + \frac{1}{C_d} \frac{\partial I}{\partial x} + \frac{\partial}{\partial x}\left(\frac{1}{C_d} \right) I = -\frac{\partial}{\partial x}\left(\frac{L_d}{R_d C_d} \right) \frac{\partial I}{\partial t} \tag{A.5}$$

while differentiating Eq. (A.2) with respect to t results in

$$\frac{\partial^2 I}{\partial x \partial t} = -G_d \frac{\partial V}{\partial t} - C_d \frac{\partial^2 V}{\partial t^2} \tag{A.6}$$

Using Equations (A.2), (A.3) and (A.6) to replace terms in Eq. (A.5) gives

$$\frac{\partial V}{\partial t} = \frac{\partial}{\partial x}\left(\frac{1}{R_d C_d} \frac{\partial V}{\partial x} \right) - \frac{G_d}{C_d} V - \frac{1}{R_d} \frac{\partial}{\partial x}\left(\frac{1}{C_d} \right) \frac{\partial V}{\partial x} + \frac{I_d}{C_d} \tag{A.7}$$

Appendix B: Steady-state I/O relationship for an exponential TL segment

Under steady-state conditions, Equations (A.2) and (A.4) for a TL simplify to

$$\frac{dV}{dx} = -IR_d \tag{B.1}$$

and

$$\frac{dI}{dx} = -G_d V + I_d \tag{B.2}$$

Differentiating both with respect to x, and then using Equations (B.1) and (B.2) to replace dI/dx and dV/dx, gives

$$\frac{d^2 V}{dx^2} = \frac{1}{R_d} \frac{dR_d}{dx} \frac{dV}{dx} + R_d G_d V - R_d I_d \tag{B.3}$$

and

$$\frac{d^2 I}{dx^2} = \frac{1}{G_d} \frac{dG_d}{dx} \frac{dI}{dx} - \frac{dG_d}{dx} \frac{I_d}{G_d} + G_d R_d I + \frac{dI_d}{dx} \tag{B.4}$$

Replacing G_d, I_d and R_d using Eq. (1.5), and simplifying, gives

$$\frac{d^2 V}{dx^2} = \frac{v}{D} \frac{dV}{dx} + \frac{K}{D} V - \frac{S}{D} \tag{B.5}$$

and

$$\frac{d^2 I}{dx^2} = -\frac{v}{D}\frac{dI}{dx} + \frac{K}{D} I \tag{B.6}$$

Equations (B.5) and (B.6) are second-order ordinary differential equations that can be solved exactly giving the I/O relationship for an exponential TL segment. Assuming that the input is at $x = 0$, the output at $x = l$, setting $V(0) = V_i$ and $I(0) = I_i$, and, in order to satisfy Equations (B.1) and (B.2),

$$\frac{dV(0)}{dx} = -I_i R_d(0), \quad \frac{dI(0)}{dx} = -G_d(0) V_i + I_d(0) \tag{B.7}$$

and solving, gives the I/O relationship

$$\begin{bmatrix} V_o \\ I_o \end{bmatrix} = \begin{bmatrix} \beta\delta - \dfrac{\beta\gamma v}{\zeta} & -\dfrac{2c\beta\gamma}{\zeta} \\ -\dfrac{2DK\gamma}{c\beta\zeta} & \dfrac{\gamma v + \delta\zeta}{\beta\zeta} \end{bmatrix} \begin{bmatrix} V_i \\ I_i \end{bmatrix} + \begin{bmatrix} \dfrac{\zeta + \beta\gamma v - \beta\delta\zeta}{K\zeta} \\ \dfrac{2D\gamma}{c\beta\zeta} \end{bmatrix} S \tag{B.8}$$

where

$$\beta = \exp\left(\frac{v}{2D}\Delta x\right), \ \gamma = \sinh\left(\frac{\zeta}{2D}\Delta x\right), \text{ and } \delta = \cosh\left(\frac{\zeta}{2D}\Delta x\right) \tag{B.9}$$

and

$$\zeta = \sqrt{v^2 + 4KD} \tag{B.10}$$

and c is the value of $1/C_d$ at the TL input end.

Appendix C: TL I/O relationships when K = 0

In a situation where the reaction coefficient is zero, Eq. (B.8) simplifies to

$$\begin{bmatrix} V_{o|n,j} \\ I_{o|n,j} \end{bmatrix} = \begin{bmatrix} 1 & \dfrac{c_{n,j} - c_{n,j}\chi_{n,j}}{v_{n,j}} \\ 0 & 1 \end{bmatrix} \begin{bmatrix} V_{i|n,j} \\ I_{i|n,j} \end{bmatrix} + \begin{bmatrix} \dfrac{\Delta x}{v_{n,j}} - \dfrac{D_{n,j}\left(\chi_{n,j} - 1\right)}{v_{n,j}^2} \\ \dfrac{D_{n,j}}{c_{n,j} v_{n,j}}\left(1 - \dfrac{1}{\chi_{n,j}}\right) \end{bmatrix} S_{n,j}$$

where

$$\chi_{n,j} = \exp\left(\frac{v_{n,j}}{D_{n,j}}\Delta x\right)$$

In a situation where both reaction and convection coefficients are zero, it becomes

$$\begin{bmatrix} V_{o|n,j} \\ I_{o|n,j} \end{bmatrix} = \begin{bmatrix} 1 & -\Delta x / D_{n,j} \\ 0 & 1 \end{bmatrix} \begin{bmatrix} V_{i|n,j} \\ I_{i|n,j} \end{bmatrix} + \begin{bmatrix} -\Delta x^2 / 2D_{n,j} \\ \Delta x \end{bmatrix} S_{n,j}$$

Appendix D: Derivation of the equation for the voltage in a 2D TL network

To derive the equation for the voltage across a two-dimensional network of interconnected vertical and horizontal transmission lines, consider a small section of such a network, of dimensions $\Delta x \times \Delta y$, as represented using lumped components in Figure 16.

Considering the voltage drop along the horizontal TL section gives

$$V - \frac{\partial V}{\partial x}\Delta x - \left(I_x - \frac{\partial I_x}{\partial x}\Delta x \right) R_{dx}\Delta x - V = 0 \tag{D.11}$$

or, as Δx approaches zero,

$$-\frac{1}{R_{dx}}\frac{\partial V}{\partial x} = I_x \tag{D.12}$$

Let the distributed capacitance at any point, whether on the TL in the x-direction or the y-direction, equal

$$C_d = C_{dx} = C_{dy} r \tag{D.13}$$

where $r = \Delta y/\Delta x$. The reason for doing this is explained below. Dividing Eq. (D.12) by C_d gives

$$-\frac{1}{R_{dx}C_d}\frac{\partial V}{\partial x} = \frac{I_x}{C_d} \tag{D.14}$$

which, when differentiated with respect to x, gives

$$-\frac{\partial}{\partial x}\left(\frac{1}{R_{dx}C_d}\frac{\partial V}{\partial x} \right) = \frac{1}{C_d}\frac{\partial I_x}{\partial x} + \frac{\partial}{\partial x}\left(\frac{1}{C_d} \right) I_x \tag{D.15}$$

Replacing I_x using Eq. (D.14) and rearranging the result gives

$$-\frac{\partial}{\partial x}\left(\frac{1}{R_{dx}C_d}\frac{\partial V}{\partial x} \right) + \frac{1}{R_{dx}}\frac{\partial}{\partial x}\left(\frac{1}{C_d} \right)\frac{\partial V}{\partial x} = \frac{1}{C_d}\frac{\partial I_x}{\partial x} \tag{D.16}$$

Similarly, for the y-direction,

$$-\frac{\partial}{\partial y}\left(\frac{1}{R_{dy}C_d}\frac{\partial V}{\partial y} \right) + \frac{1}{R_{dy}}\frac{\partial}{\partial y}\left(\frac{1}{C_d} \right)\frac{\partial V}{\partial y} = \frac{1}{C_d}\frac{\partial I_y}{\partial y} \tag{D.17}$$

The sum of the currents entering the junction of the two TLs equals zero, and so

$$\begin{aligned} &\left(I_x - \frac{\partial I_x}{\partial x}\Delta x \right) + \left(I_y - \frac{\partial I_y}{\partial y}\Delta y \right) + I_{dx}\Delta x + I_{dy}\Delta y - \left(G_{dx}\Delta x + G_{dy}\Delta y \right) V \ldots \\ &\qquad \ldots - \left(C_{dx}\Delta x + C_{dy}\Delta y \right)\frac{\partial V}{\partial t} = I_x + I_y \end{aligned} \tag{D.18}$$

which simplifies to

$$\left(C_{dx}\Delta x + C_{dy}\Delta y \right)\frac{\partial V}{\partial t} = -\frac{\partial I_x}{\partial x}\Delta x - \frac{\partial I_y}{\partial y}\Delta y + I_{dx}\Delta x + I_{dy}\Delta y - \left(G_{dx}\Delta x + G_{dy}\Delta y \right) V \tag{D.19}$$

Using Equations (D.16) and (D.17) to replace the derivatives of the currents, and using $r\Delta x = \Delta y$ to simplify the result, gives

$$\begin{aligned} &\left(C_{dx} + C_{dy} r \right)\frac{\partial V}{\partial t} = C_d \frac{\partial}{\partial x}\left(\frac{1}{R_{dx}C_d}\frac{\partial V}{\partial x} \right) + C_d r \frac{\partial}{\partial y}\left(\frac{1}{R_{dy}C_d}\frac{\partial V}{\partial y} \right) - \frac{C_d}{R_{dx}}\frac{\partial}{\partial x}\left(\frac{1}{C_d} \right)\frac{\partial V}{\partial x} \ldots \\ &\qquad \ldots - \frac{C_d r}{R_{dy}}\frac{\partial}{\partial y}\left(\frac{1}{C_d} \right)\frac{\partial V(x,y,t)}{\partial y} - \left(G_{dx} + G_{dy} r \right) V + I_{dx} + I_{dy} r \end{aligned} \tag{D.20}$$

Since, from Eq. (D.13), $C_{dx} + C_{dy} r = 2C_d$, this can be rewritten as

$$
\begin{aligned}
\frac{\partial V}{\partial t} &= \frac{\partial}{\partial x}\left(\frac{1}{2R_{dx}C_d}\frac{\partial V}{\partial x}\right) + r\frac{\partial}{\partial y}\left(\frac{1}{2R_{dy}C_d}\frac{\partial V}{\partial y}\right) - \frac{1}{R_{dx}}\frac{\partial}{\partial x}\left(\frac{1}{2C_d}\right)\frac{\partial V}{\partial x}\dots \\
&\dots - \frac{r}{R_{dy}}\frac{\partial}{\partial y}\left(\frac{1}{2C_d}\right)\frac{\partial V\left(x,y,t\right)}{\partial y} - \left(\frac{G_{dx}+G_{dy}r}{2C_d}\right)V + \frac{I_{dx}+I_{dy}r}{2C_d}
\end{aligned}
\qquad \text{(D.21)}
$$

This has the same form as the equation for convection-reaction-diffusion in two-dimensions (with non-conservative convection terms). That would not be the case if the condition in Eq. (D.13) was not satisfied.

References

1. Salas, A.H., L.J.M. H, and O.F. S, *Reaction-diffusion equations: A chemical application.* Scientia et Technica, 2010. **XVII**(46): p. 134-137

2. Volpert, V. and S. Petrovskii, *Reaction-diffusion waves in biology.* Physics of Life Reviews, 2009. **6**(4): p. 267-310.

3. Eslamian, M. and M.Z. Saghir, *Thermodiffusion (thermomigration) and convection in molten semiconductor-metal layers.* International Journal of Thermal Sciences, 2011. **50**(7): p. 1232-1242.

4. Al-zeben, M.Y., A.H.M. Saleh, and M.A. Al-Omar, *TLM modelling of diffusion, drift and recombination of charge carriers in semiconductors.* International Journal for Numerical Modelling, 1992. **5**(1992): p. 219 - 225.

5. Guin, L.N., *Existence of spatial patterns in a predator-prey model with self-and cross-diffusion.* Applied Mathematics and Computation, 2014. **226**(0): p. 320-335.

6. Rodrigo, M.R.M., Rogemar S., *An alternative approach to solving the Black-Scholes equation with time-varying parameters.* Applied Mathematics Letters, 2006. **19**(4): p. 398-402.

7. Cen, Z. and A. Le, *A robust and accurate finite difference method for a generalized Black-Scholes equation.* Journal of Computational and Applied Mathematics, 2011. **235**(13): p. 3728-3733.

8. Kuang, S., et al., *CFD modeling and analysis of the multiphase flow and performance of dense medium cyclones.* Minerals Engineering, 2014. **62**(0): p. 43-54.

9. Chaabane Khelifi, S., et al., *A hybrid multigrid method for convection–diffusion problems.* Journal of Computational and Applied Mathematics, 2014. **259, Part B**(0): p. 711-719.

10. Duffy, D.G., *Solutions of partial differential equations*. First ed. 1986: TAB Professional and Reference books.

11. Gockenback, M.S., *Partial differential equations: Analytical and numerical methods*. Second ed. 2011: siam.

12. Majumdar, P., *Computational methods for heat and mass transfer*. 2005, New York, London: Taylor & Francis.

13. Versteeg, H.K. and W. Malalasekera, *An introduction to computational Fluid Dynamics. The Finite Volume Method*. 1995, Harlow: Pearson Education Limited.

14. Vaidya, D.S., et al., *Convection-diffusion of solutes in media with piecewise constant transport properties.* Chemical Engineering Science, 1996. **51**(24): p. 5299-5312.

15. Lee, C., J. Dolbow, and P.J. Mucha, *A narrow-band gradient-augmented level set method for multiphase incompressible flow.* Journal of Computational Physics, 2014. **273**(0): p. 12-37.

16. Nicolas Fiétiera, Y.K., Matthieu Vialard, *New methods for the fast simulations of the extrusion process of hot metals.* Journal of Materials Processing Technology, 2009. **209**(5): p. 2244 - 2259.

17. Mroginski, J.L., et al., *A finite element approach for multiphase fluid flow in porous media.* Mathematics and Computers in Simulation, 2010. **81**(1): p. 76-91.

18. Kennedy, A. and W.J. O'Connor, *A TLM method for steady-state convection-diffusion: Some additions and refinements.* International Journal of Numerical Methods in Engineering, 2009. **77**(4): p. 518-535.

19. Murthy, J.Y., *Numerical Methods in Heat, Mass, and Momentum Transfer*. 2002, School of Mechanical Engineering Purdue University. p. 1 - 196.

20. Baruch, G., G. Fibich, and S. Tsynkov, *High-order numerical method for the nonlinear Helmholtz equation with material discontinuities in one space dimension.* Journal of Computational Physics, 2007. **227**(1): p. 820-850.

21. Al-Sanea, S.A., M.F. Zedan, and S.N. Al-Hussain, *Effect of thermal mass on performance of insulated building walls and the concept of energy savings potential.* Applied Energy, 2012. **2012**(89): p. 430 - 442.

22. Kumar, R. and J. Kumar, *Numerical simulation and convergence analysis of a finite volume scheme for solving general breakage population balance equations.* Applied Mathematics and Computation, 2013. **219**(10): p. 5140-5151.

23. Grigoriev, M.M. and G.F. Dargush, *Boundary element methods for transient convective diffusion. Part I: General formulation and 1D implementation.* Computer Methods in Applied Mechanics and Engineering, 2003(192): p. 4281-4298.

24. Nadukandi, P., E. Oñate, and J. Garcia, *A high-resolution Petrov-Galerkin method for the 1D convection-diffusion-reaction problem.* Computer Methods in Applied Mechanics and Engineering, 2010(199): p. 525-546.

25. Hoffman, J.D., *Numerical methods for engineering and scientists*. 1992, McGraw-Hill, Inc.

26. S. R. Idelsohn, J.C.H.a.E.O., *Petrov-Galerkin methods for the transient advective-diffusive equation with sharp gradients.* Internationa journal for numerical methods in engineering, 1996. **39**: p. 1455 - 1473.

Table 1: The values plotted in Figure 9(b) and corresponding estimates of the order of convergence.

N	LCM	FVM_{QUICK}
5	30.741299	30.134557
9	30.785471	30.441016
17	30.796159 **2.0**	30.619494 **0.8**
33	30.799386 **1.7**	30.708041 **1.0**
65	30.800234 **1.9**	30.754718 **0.9**
129	30.800448 **2.0**	30.761570 **2.8**
257	30.800501 **2.0**	30.783930 **-1.7**

Table 2: The values plotted in Figure 11(b) and corresponding estimates of the order of convergence.

N	LCM	FVM_{CD}
7	0.115150	0.110058
13	0.114826	0.112876
25	0.114835 **5.1**	0.114104 **1.2**
49	0.114842 **0.5**	0.114548 **1.5**
97	0.114843 **2.2**	0.114715 **1.4**
193	0.114844 **2.3**	0.114784 **1.3**

Table 3: Values of $V(0.5, 0.5; 0.02)$ for Test 3 calculated using different numbers of nodes, and corresponding estimates of the order of convergence.

N	LCM
5×5	0.104826
9×9	0.100109
17×17	0.098548 **1.6**
33×33	0.098077 **1.7**
65×65	0.097958 **2.0**
129×129	0.097931 **2.1**

Sabawoon Shafaq, Figure 1

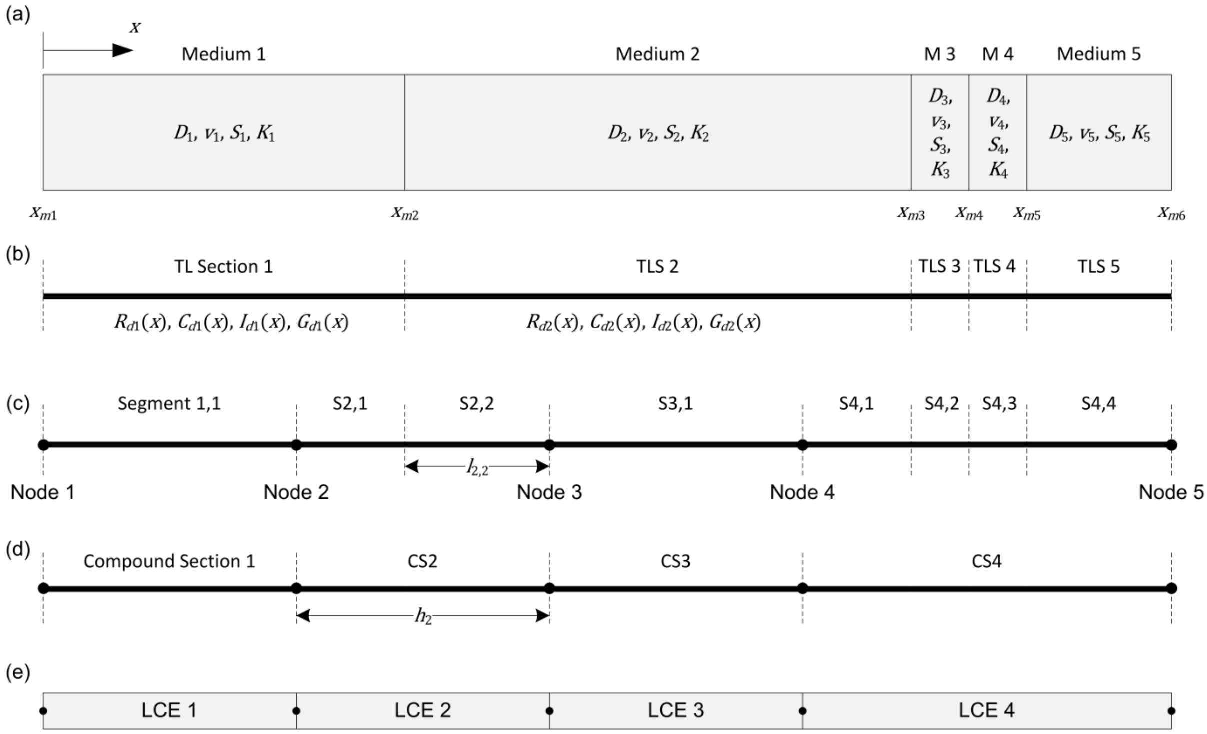

Figure 1: Physical domain with piecewise-constant properties of media, (a), analogous TL composed of exponential transmission line sections, (b), position of nodes along the domain at which the solution is sought and exponential TL segments, (c), compound TL sections linking nodes comprising of one or more exponential TL segments,(d), and the lumped-component circuit elements used to model the TL in the lumped-component circuit method, (e).

Sabawoon Shafaq, Figure 2

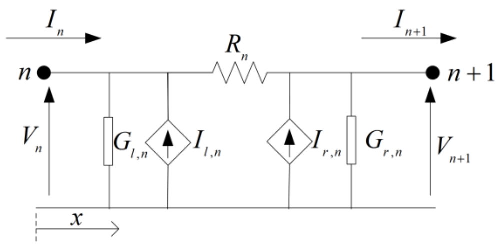

Figure 2: Lumped-component circuit element (LCE).

Sabawoon Shafaq, Figure 3

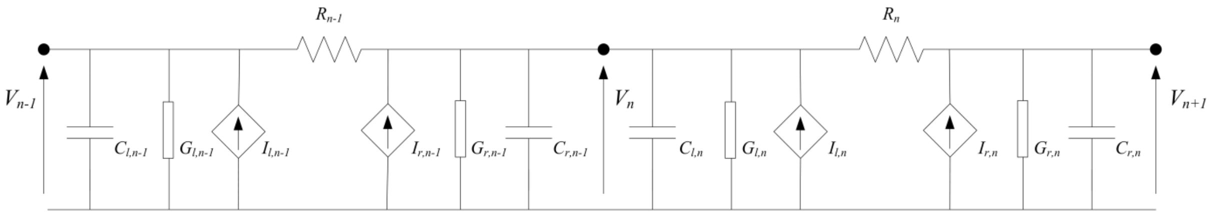

Figure 3: Two LCEs and three nodes in a lumped-component circuit model.

Sabawoon Shafaq, Figure 4

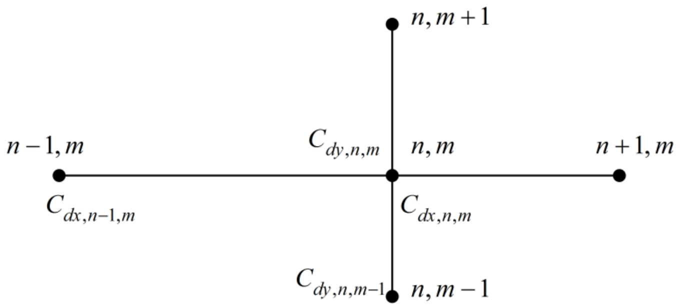

Figure 4: Part of a 2D TL network around node *n*, *m*. The values of the distributed capacitance of the horizontal and vertical lines at node *n*, *m* are indicated.

Sabawoon Shafaq, Figure 5

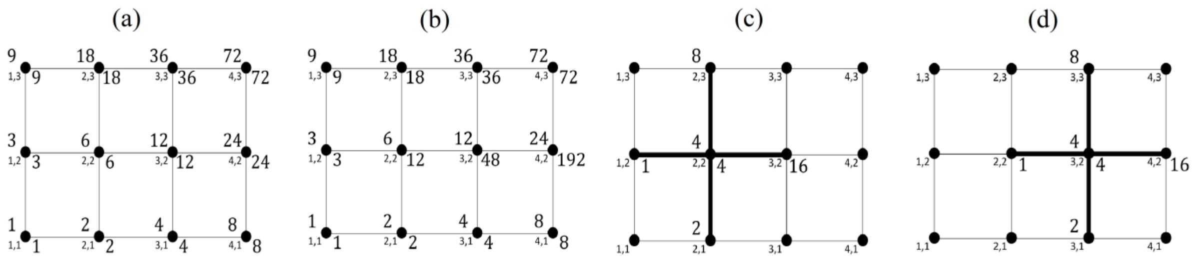

Figure 5: Twelve nodes in 2D models with possible values indicated below and to the right of each node and values indicated above and to the left.

Sabawoon Shafaq, Figure 6

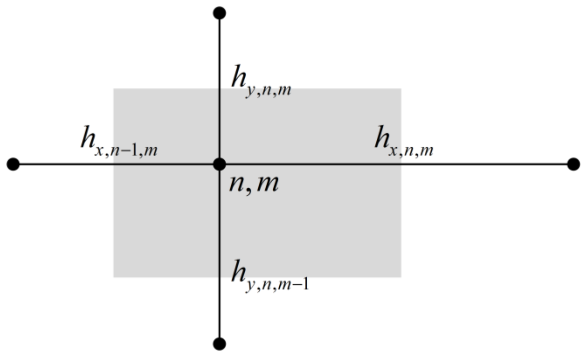

Figure 6: The rectangular area corresponding to node *n*, *m* in an unevenly spaced grid, with node-spacings indicated

Sabawoon Shafaq, Figure 7

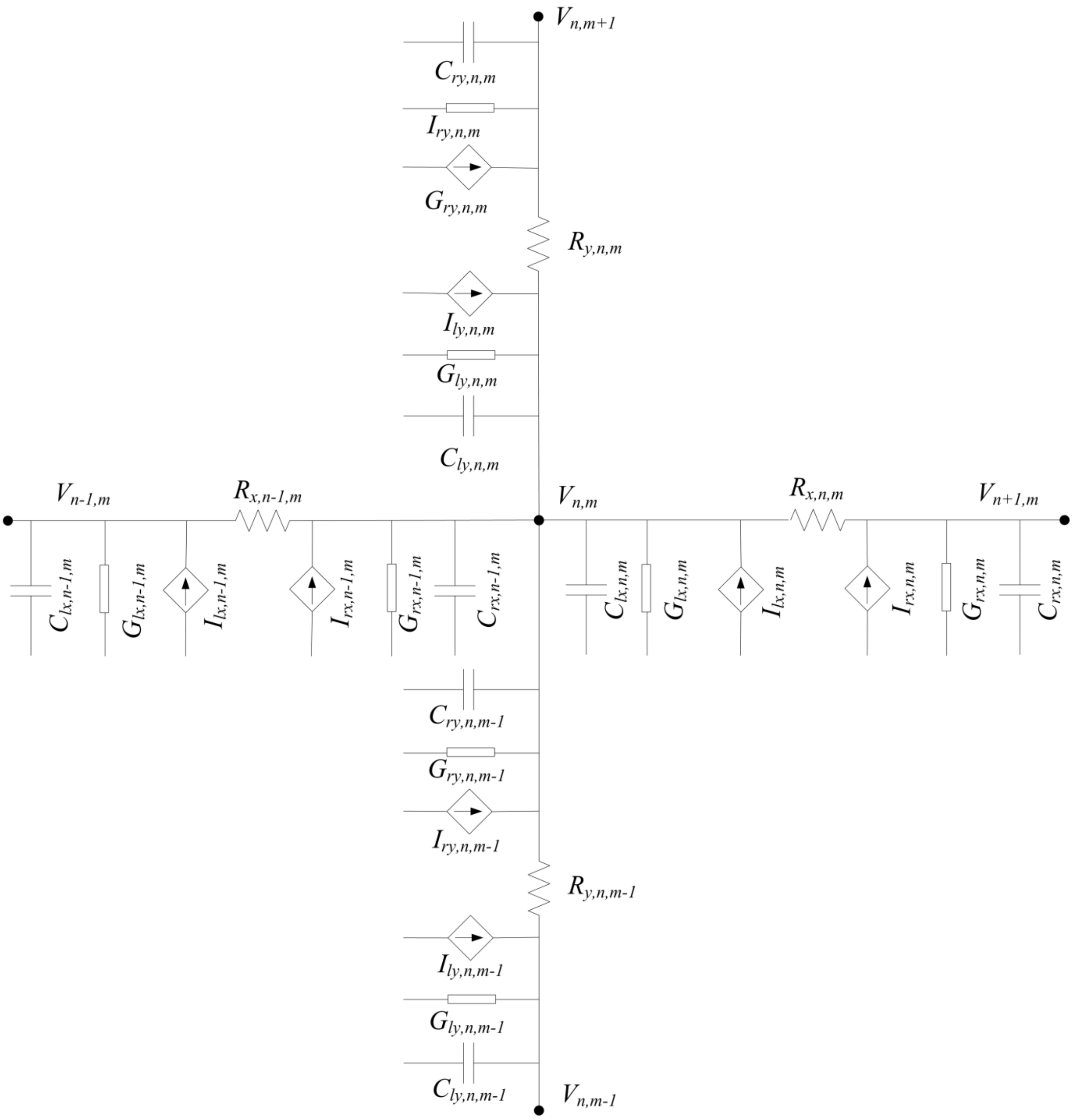

Figure 7: Part of a 2D lumped-component circuit model.

Sabawoon Shafaq, Figure 8

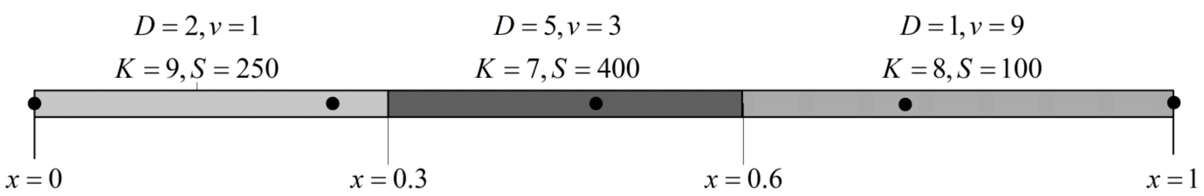

Figure 8: Test 1 problem geometry and coefficients and the positions of $N = 5$ evenly spaced nodes.

Sabawoon Shafaq, Figure 9

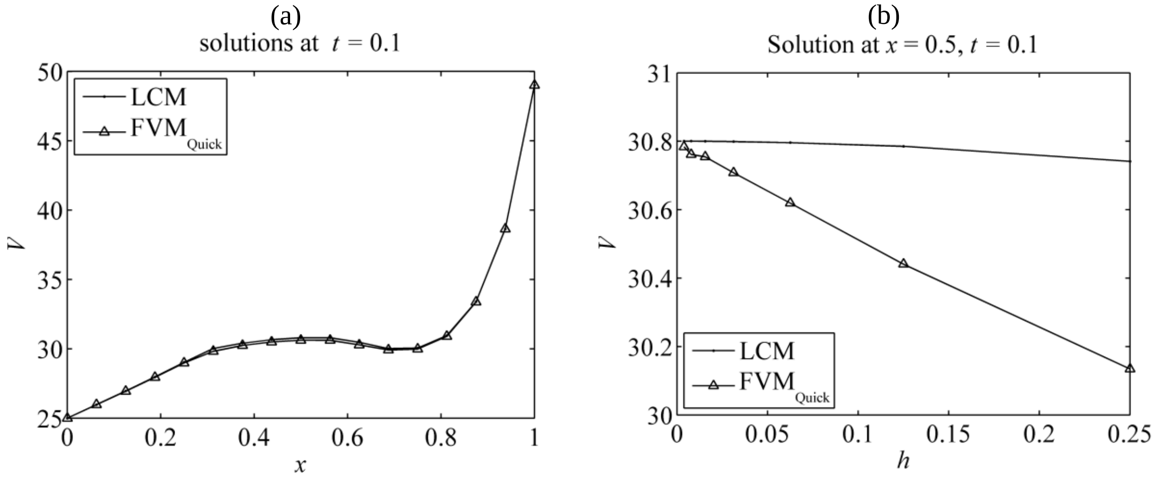

Figure 9: Solution of Test 1 problem using a model with N = 17 nodes, (b), and the convergence of the solution as h approaches zero, (b).

Sabawoon Shafaq, Figure 10

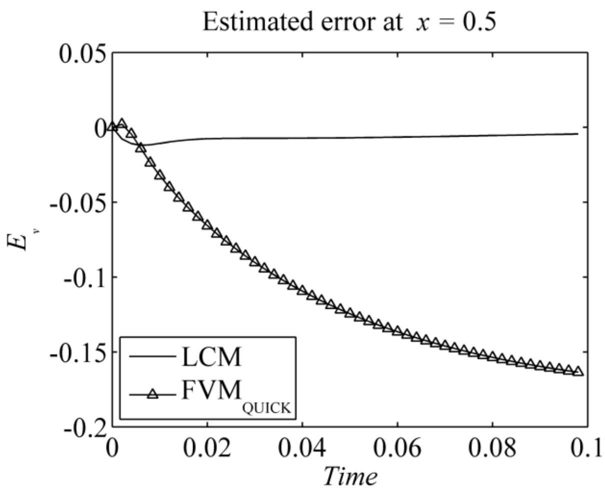

Figure 10: Estimated error in the solution, at the midpoint of the domain, plotted over time.

Sabawoon Shafaq, Figure 11

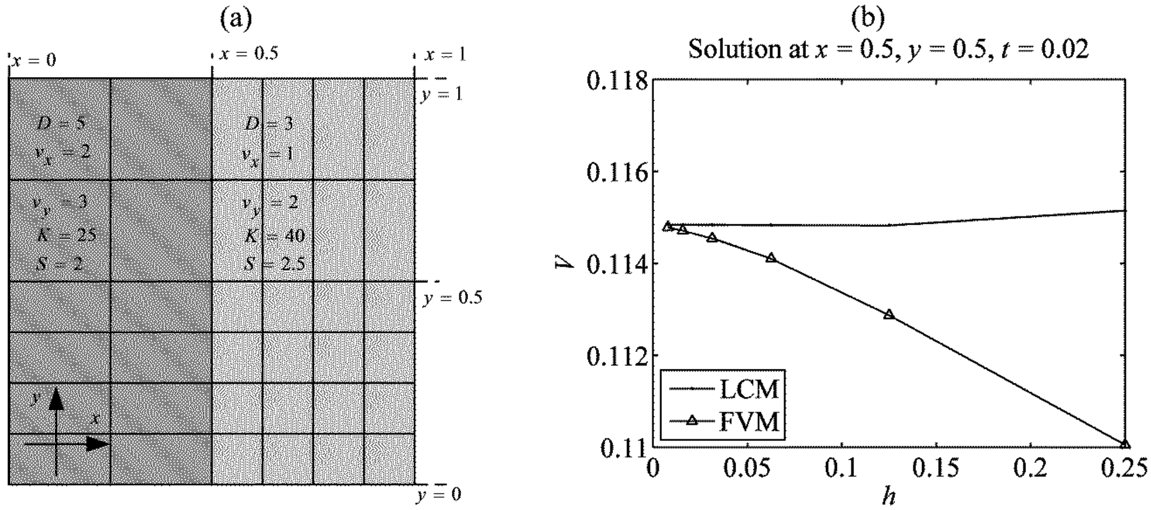

Figure 11: Test 2 problem geometry and coefficients and a 7×7 grid of nodes, (a), and estimated values of $V(0.5, 0.5; 0.02)$ plotted against h, (b).

Sabawoon Shafaq, Figure 12

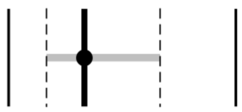

Figure 12: Three vertical transmission lines in a domain. The coefficients for the highlighted TL at the point indicated are averages of the problem coefficients along the grey line.

Sabawoon Shafaq, Figure 13

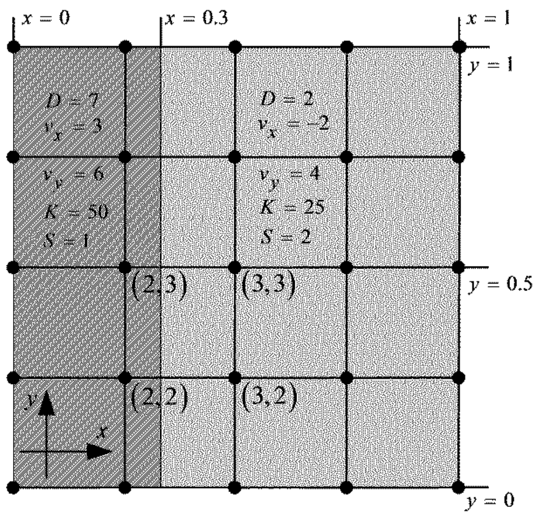

Figure 13: Test 3 problem geometry and coefficients and a 5×5 grid of nodes.

Sabawoon Shafaq, Figure 14

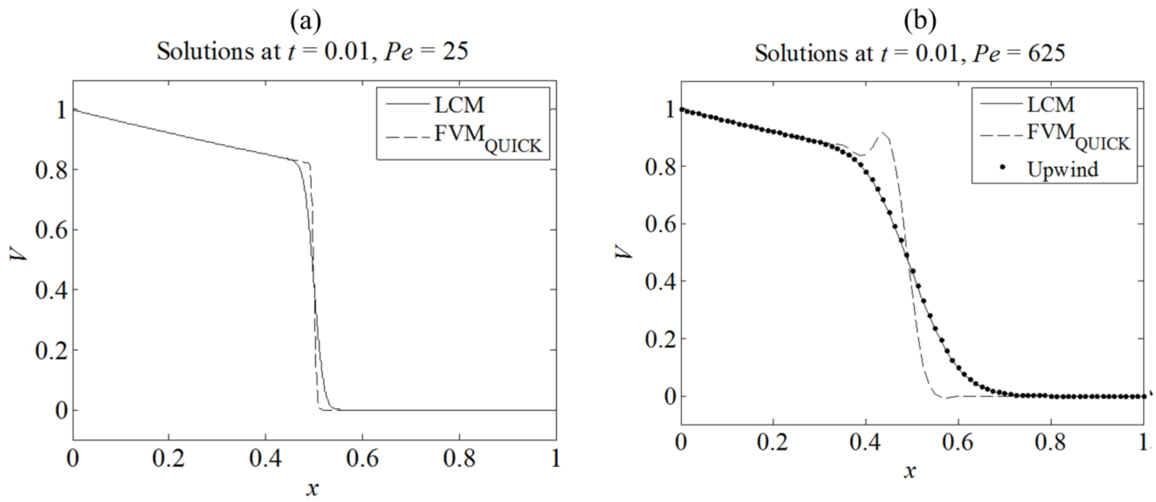

Figure 14: Solutions of Test 4 problem using models with N = 2001 nodes, (a), and models with N = 81 nodes, (b).

Sabawoon Shafaq, Figure 15

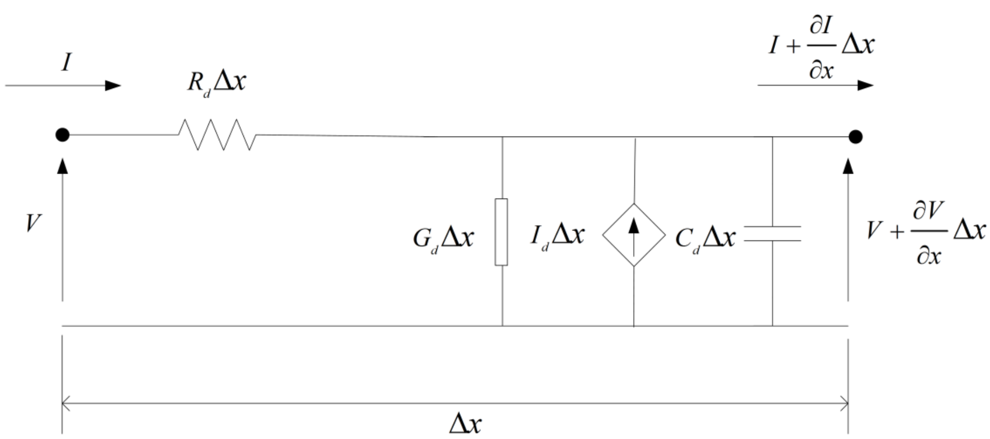

Figure 15: A short section of uniform TL of length Δx.

Sabawoon Shafaq, Figure 16

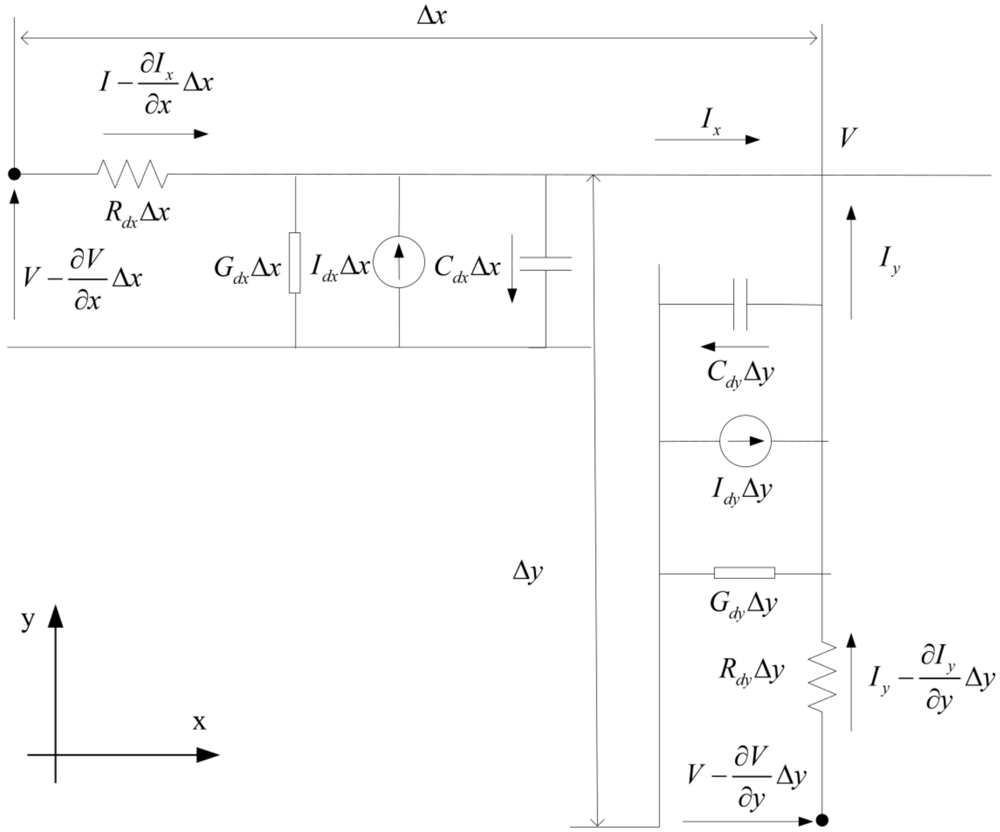

Figure 16: A small segment of a 2D TL network with distributed properties represented by lumped components. The diagram shows only one conductor in each TL connected at a point, but the second conductors are also connected; that connection is not shown to make the diagram as clear as possible.